

AD-A199 379

C S S A

DIRECTIONALITY OF CONTINUUM GAMMA RAYS
FROM SOLAR FLARES

TAEIL BAI

Center for Space Science and Astrophysics

CSSA-ASTRO-88-02
1988 April



CENTER FOR SPACE SCIENCE AND ASTROPHYSICS
STANFORD UNIVERSITY
Stanford, California

DTIC
ELECTE
AUG 3 1 1988
S H D

DISTRIBUTION STATEMENT A

Approved for public release;
Distribution Unlimited

88 8 18 020

4

DIRECTIONALITY OF CONTINUUM GAMMA RAYS
FROM SOLAR FLARES

TAEIL BAI

Center for Space Science and Astrophysics

CSSA-ASTRO-88-02
1988 April

To appear in the *Astrophysical Journal* (Vol. 334 ; 1988 November 15)

NASA grant NGL 05-020-272
Office of Naval Research Contract N00014-85-K-0111
NASA Contract NAS8-37334 (subcontracted with Lockheed)

DISTRIBUTION STATEMENT A
Approved for public release;
Distribution Unlimited

DTIC
ELECTE
AUG 31 1988
S D
H

DIRECTIONALITY OF CONTINUUM GAMMA RAYS
FROM SOLAR FLARES

TAEIL BAI

Center for Space Science and Astrophysics, Stanford University

ABSTRACT

Using the hard X-ray spectrometer total counts as calibration, I investigate how the brightness of γ -rays above 300 keV changes as a function of the heliocentric angle of a flare. The normalized γ -ray brightness, on the average, increases with the heliocentric angle; a flare at the limb is estimated to be 13 times brighter in γ -rays than a similar flare near the central meridian. Both pancake-like electron distributions and downward beam distributions can be adjusted to produce the deduced limb brightening.

I. INTRODUCTION

Radiation from energetic electrons is directional, with more radiation being emitted in the forward direction. The more energetic the electron, the more directional the radiation becomes. In solar flares some of the hard X-ray photons emitted toward the photosphere are backscattered via Compton scattering and the rest are consumed in photoionization (Langer and Petrosian 1977; Bai and Ramaty 1978). Backscattered photons tend to diminish the directionality of observed hard X-rays; hence, the directionality of hard X-rays may be detectable only at high energies >100 keV, depending on the distribution of electrons (Bai and Ramaty 1978; Leach and Petrosian 1983). Therefore, the anisotropy of hard X-rays and γ -

rays from solar flares can yield information on the angular distribution of the momenta of energetic electrons.

There are several ways to study the anisotropy of solar hard X- and γ -rays. One is to study the distribution on the disk of the Sun of flares that are detected with a certain detector. Suppose that more radiation is emitted in the directions parallel to the surface of the Sun than in the vertical direction. Then, a flare located near the limb will look brighter than the same flare located near the disk center. This effect is called "limb brightening." Limb brightening will in turn push above the detection threshold many limb flares which would not be detected were they located near the disk center. Distributions of flares detected with hard X-ray detectors have been studied (Kane 1974; Datlowe *et al.* 1977). But because of the effect of Compton backscatter, the limb brightening is negligible at the photon energies in their studies, even if the electron distribution is anisotropic (Bai and Ramaty 1978; Langer and Petrosian 1977; Leach and Petrosian 1983). Hence, one could not draw any firm conclusions from their studies. However, at higher energies the anisotropy is detectable, if the electron distribution shows a reasonable degree of anisotropy. Vestrand *et al.* (1987) studied the distribution of flares detected with the gamma ray spectrometer (GRS) aboard the *Solar Maximum Mission (SMM)* whose threshold energy is 300 keV. They found that more flares are detected near the limb than are expected from an isotropic radiation case. The excess of limb flares is at the 2.5σ level. Such limb brightening can be caused either by electrons streaming down toward the photosphere or by electrons with pancake-like momentum distributions (Dermer and Ramaty 1986).

The second way of studying the momentum distributions of energetic electrons is to investigate photon spectra. Because the anisotropy of

radiation increases with increasing photon energy for a given electron momentum distribution, the photon spectrum of a given flare will vary depending on its location on the Sun. By studying the γ -ray continuum spectrum of the GRS events, Vestrand *et al.* (1987) found that the γ -ray spectrum on the average becomes flatter as the location of flares is closer to the limb. This effect is significant at a 3.4σ level. The observed spectral behavior is also consistent with either downward beam distributions or pancake-like momentum distributions.

The third way of studying the momentum distributions of energetic electrons is to observe the same flares at different viewing angles. If we have two identical hard X-ray detectors observing the Sun at widely separate angles, the task of unraveling the radiation pattern will be rather simple. But stereoscopic observations analyzed by Kane *et al.* (1988) were made with two different detectors with different efficiencies and energy channels. Therefore, a large number of flares are needed to compensate for such deficiency. Kane *et al.* (1988) analyzed 39 flares commonly observed without limb occultation by the hard X-ray detectors aboard the *Pioneer Venus Orbiter (PVO)* and the third *International Sun-Earth Explorer (ISEE 3; now ICE)*. According to Kane *et al.* (1988), the observed anisotropy is much smaller than what is expected from model calculations made by Petrosian (1985) and Dermer and Ramaty (1986) to fit the GRS flare distribution obtained by Vestrand *et al.* (1987). In short, the results of Kane *et al.* require a much lower degree of anisotropy, if any, than those of Vestrand *et al.*

II. ANALYSIS



For		<input checked="" type="checkbox"/>
a		<input type="checkbox"/>
Justification		<input type="checkbox"/>
By <i>per letter</i>		
Distribution/		
Availability Codes		
Dist	Avail and/or Special	
<i>A-1</i>		

In order to help resolve this conflict, I have made the following study. Because of Compton backscatter, the directionality of 30 keV photons is negligible, even if the electron distribution is highly anisotropic (Bai and Ramaty 1978; Leach and Petrosian 1983). Since the threshold energy of the hard X-ray burst spectrometer (HXRBS) is about 30 keV, we can use the HXRBS total counts as a calibrator in evaluating the directivity of γ -ray continuum emission.

Figure 1 shows the correlation between HXRBS total counts, X , and GRS fluences, Y , for flares observed with GRS aboard *SMM* between 1980 February and 1985 December. GRS fluences are time integrated flux of γ -rays above 300 keV. GRS fluences are evaluated from the formula

$$Y=A 0.3^{-(\delta-1)/(\delta-1)} \quad (1)$$

where A is the differential γ -ray fluence at 1 MeV and δ is the spectral index given in Table 1 of Vestrand *et al.* HXRBS total counts are taken from Dennis *et al.* (1985). Solid dots in Figure 1 indicate disk flares, and "+" marks indicate limb flares. To be consistent with Vestrand *et al.*, flares with heliocentric angle greater than 64 degrees are defined as limb flares.

In order to determine the limb brightening of γ -rays above 300 keV, one can make least square fits to the data points in Figure 1. The GRS flares are selected by virtue of emitting γ -rays above the GRS threshold. Because HXRBS total counts and GRS fluences have a positive correlation, many flares with small HXRBS total counts did not emit detectable γ -rays. To remove the bias of the data set due to the GRS threshold effect, I first selected flares with HXRBS total counts greater than 6×10^5 in making the fits. There are 60 flares meeting this requirement. Second, even among flares with HXRBS total counts greater than 6×10^5 some were not detected by the GRS. To compensate for this, I weighted the flares with GRS fluences

below 10 photons cm^{-2} by the inverse of the detectability function. The γ -ray size distribution function, $N(Y)$, which shows the number of flares above a given γ -ray fluence Y , is well fitted by a power law down to $Y=10$ photons cm^{-2} (e.g., Chupp 1984). The deviation from the power law below 10 photons cm^{-2} is assumed to be caused by the detectability.

After these two procedures I determined parameters α and β which minimize the quantity

$$S = \sum_{i=1}^n (y_i - \alpha - \beta x_i)^2 \quad (2)$$

where $x_i = \log_{10} (X_i / 10^5)$ and $y_i = \log_{10} Y_i$, X_i is the HXRBS total count, and Y_i is the GRS fluence of the i th flare. Parameters α and β are determined for disk flares and limb flares separately. The linear regression line thus obtained for disk flares is

$$y_d = 1.04x, \quad (3)$$

and it is shown by the solid line. The linear regression line for limb flares is

$$y_l = 0.74 + 0.92x, \quad (4)$$

and is shown by the dashed line. Notice here that the latter is located higher than the former. For $x=1$, $\Delta y = y_l - y_d = 0.62$; this means that at $X=10^6$ counts limb flares are brighter in γ rays by a factor $f=10^{0.62}=4.2$. Similarly, at $X=10^7$ counts limb flares are brighter in γ rays by a factor of 3.2. The change of the brightening factor with X is due to the difference in slopes of equations (3) and (4). However, this difference is not statistically significant. Therefore, we can say that limb flares are brighter in γ -rays than disk flares by about 3.5 on the average.

One can make least-squares fits by minimizing the quantity

$$S_x = \sum_{i=1}^n (x_i - C - Dy_i)^2 \quad (5)$$

The regression line obtained with equation (2) can be used to estimate the expected γ -ray fluence for a given value of HXRBS total counts. On the other hand, the regression line obtained with equation (5) can be used to estimate the expected HXRBS total counts for a given value of γ -ray fluence. Therefore, equation (2) is physically more meaningful in determining the γ -ray brightening factor. However, equation (5) is more advantageous in that we do not have to worry about the GRS threshold effect. The linear regression line thus obtained for disk flares is

$$y_d = 0.20 + 1.18x, \quad (6)$$

and that for limb flares is

$$y_l = 0.06 + 1.61x. \quad (7)$$

From equations (6) and (7) we estimate the limb brightening factor of γ rays to be 2.0 for $x=1$ ($X=10^6$ counts) and 5.2 for $X=10^7$ counts. These estimates are in rough agreement with those obtained from equations (3) and (4).

I have done a similar analysis by using HXRBS peak rates instead of HXRBS total counts. The results are very similar.

Not only are the GRS fluences and HXRBS total counts positively correlated but also the coefficients of the regression lines given by equations (2) and (3) are almost equal to unity. Therefore, we can with some confidence normalize the GRS fluences by dividing by their HXRBS total counts. I define the quantity k as

$$k = \log_{10}(10^5 Y/X) \quad (8)$$

where Y is the GRS fluence above 300 keV and X is the HXRBS total count. This quantity is plotted against the heliocentric angle θ in Figure 2. The straight line is the best fit to the data, which is expressed by

$$k = 0.27 + 0.0147(\theta - 51). \quad (9)$$

The correlation coefficient r between θ and k is 0.39 for 60 data points. (Here I used the same criterion for the selection of flares and the same weighting as in obtaining the regression lines shown in Fig. 1.) The chance for 60 pairs of uncorrelated values to have $r > 0.39$ is only 0.2%. The uncertainty in the estimate of the coefficient 0.0147 is 0.0041; therefore, the hypothesis that γ -ray emission above 300 keV is not directional is ruled out at the 3.6σ level ($0.0147/0.0041=3.6$). The γ -ray brightening factor increases on the average as flares move out from the disk center to the limb. A flare at the limb is expected to be brighter in γ rays on the average by a factor $f = 10^{0.0147(90-51)} = 12.7$ than the same flare at the central meridian ($l=0^\circ$, $b=15^\circ$). (The heliocentric angle is given by the expression $\theta = \arccos(\cos l \cos b)$, where l is the longitude and b is the latitude. Because flares seldom occur near the equator, few flares have θ values less than 15 degrees.)

The center-to-limb variation function f can be obtained from equation (9):

$$f(\theta) = 10^{0.0147(\theta-51)}, \quad (10)$$

where f is normalized to 1 at $\theta = 51^\circ$, the mean heliocentric angle of the flares used in the analysis. If we remove the center-to-limb variation by dividing GRS fluences by $f(\theta)$, the correlation coefficient between GRS fluences and HXRBS total counts increases from 0.49 to 0.54. The correlation diagram between the GRS fluences divided by $f(\theta)$ and HXRBS total counts is shown in Figure 4. We find that Figure 4 shows much less scatter than Figure 1. The scatter in Figure 4 is mostly due to variability of individual flares. The electron spectrum varies from flare to flare, and the anisotropy of energetic electrons may vary from flare to flare.

Dermer and Ramaty (1986) calculated the directionality of bremsstrahlung of energetic electrons for various electron distributions described by the following two distribution functions. The first represents downward beam distributions:

$$M_r(\cos \alpha) = \frac{r \exp(r \cos \alpha)}{2\pi[\exp(r) - \exp(-r)]} \quad (10)$$

where α is the angle with respect to the vertical direction. The larger the value of r , the larger the anisotropy. The other represents pancake-like distributions:

$$M_p(\cos \alpha) = \frac{(p+1)!!}{4\pi p!!} \sin^p \alpha. \quad (11)$$

Using Figure 14 of Dermer and Ramaty (1986), which is for a power-law electron energy spectrum with a power index 3.5, I plot in Figure 3 the center to limb variations for a downward beam distribution of $r=3$ and a pancake-like distribution of $p=6$. Two straight lines with a slope 0.0147 (the same as that of the straight line in Fig. 2) are plotted for comparison. We find that these results are compatible with the data shown in Figure 2. Although the shapes of the curves for $r=3$ and $p=6$ are different, the data points of Figure 2 have too large scatter to determine which case is better.

III. DISCUSSION AND CONCLUSION

By using HXRBS total counts as calibration, I have studied the directionality of γ rays above 300 keV. The normalized γ -ray limb brightness increases as the heliocentric angle θ of a flare increases. Flares at the limb ($\theta=90^\circ$) are brighter by 13 times on the average than similar flares at the central meridian ($\theta=15^\circ$). This behavior can be explained by either pancake-like distributions or downward beam distributions of electrons used by Dermer and Ramaty (1986).

There are several ways to study the directionality of energetic electrons accelerated by solar flares. The first is to compare the number of γ -ray flares near the disk center with that near the limb (Vestrand *et al.* 1987; Rieger *et al.* 1983). The second is to study how the spectral indices of hard X-rays and γ -rays change with θ (Bogovalov *et al.* 1985; Vestrand *et al.* 1987). The third is to observe flares at different viewing angles (Kane *et al.* 1988). Vestrand *et al.* have shown that there are more limb flares than expected from an isotropic γ -ray emission pattern. Rieger *et al.* have shown that flares with detectable γ -ray continuum above 10 MeV are all located near the limb ($\theta > 60^\circ$). This requires that relativistic electrons with energies > 10 MeV be distributed anisotropically (Dermer and Ramaty 1986). Bogovalov *et al.* have shown that the spectral index of hard X-rays above 50 keV decreases systematically with increasing θ . Vestrand *et al.* have also shown a similar behavior for the spectral index of γ -rays above 300 keV. These results of different investigators using different methods all point to anisotropic distributions of energetic electrons.

In order to deduce the distribution function of energetic electrons from the number distribution of flares, one has to perform detailed calculations of bremsstrahlung and analyze the size distribution of flares (Petrosian 1985; Dermer and Ramaty 1986; Dermer 1987). The result of Dermer and Ramaty (1986) shows that center-to-limb variations larger than 10 are required to be consistent with the excess γ -ray flares near the limb observed by Vestrand *et al.* Petrosian's (1985) calculation also shows that the center-to-limb variation is larger than 10 at 300 keV. Dermer and Ramaty have found that the observed spectral hardening of limb flares is consistent with $r=5$ for a beam distribution and $p>1$ for a pancake

distribution. However, stereoscopic observations of Kane *et al.* show that the center-to-limb variation of >300 keV γ -rays is only about 2.5 or less.

In the present paper, I normalized GRS fluences with HXRBS total counts to study the anisotropy of γ -rays. This method is superior to counting limb flares and disk flares in the following two scores. First, in this method we do not have to consider the size distribution to find out the center-to-limb variation. Second, in this method we utilize a pair of values for each flare while in the number counting method we reduce all the data to just two numbers. In these respects, a study of spectral index as a function of θ is superior to the number counting method.

The present study shows that the center-to-limb variation of γ -rays above 300 keV is larger than 10, which is consistent with the results of Petrosian (1985) and Dermer and Ramaty (1986). Among recent studies of solar γ -ray anisotropy, only the result of Kane *et al.* is consistent with a nearly isotropic distribution of energetic electrons. At present, the reason for this discrepancy is not known. However, considering that independent groups of authors using different methods obtain consistent results, except for Kane *et al.* (1988), I favor anisotropic electron distributions that can produce limb brightening.

If we acquire γ -ray data with larger dynamic ranges, perhaps with *Solar A*, the planned Japanese satellite, we will be able to determine the limb brightening factor with better confidence and better accuracy.

This research was funded by ONR Contract N00014-85-K-0111, by NASA Grant NGL 05-020-272, and as part of Solar-A collaboration under NASA Contract NAS8-37334 with Lockheed Palo Alto Research

Laboratories. The author thanks Dr. C. Dermer for providing numerical results which were published as Figures of Dermer and Ramaty (1986).

REFERENCES

- Bai, T., and Ramaty, R 1978, *Ap. J.*, **219**, 705.
- Bogovalov, S. V., *et al.* 1985, *Sov. Astron. Lett.*, **11**, 322.
- Chupp, E. L. 1984, *Ann. Rev. Astron. Ap.*, **22**, 359.
- Datlowe, D. W., O'Dell, S. L., Peterson, L. E., and Elcan, M. J. 1977, *Ap. J.*, **212**, 516.
- Dennis, B. R., Orwig, L. E., Kiplinger, A. L., Gibson, B. R., Kennard, G. S., and Tolbret, A. K. 1985, *NASA TM 86236*, (NASA: Washington, D. C.)
- Dermer, C. D. 1987, *Ap. J.*, **323**, 795.
- Dermer, C. D., and Ramaty, R 1986, *Ap. J.*, **301**, 962.
- Kane, S.R. 1974, in *IAU Symposium 57, Coronal Disturbances*, ed. G. Newkirk, Jr. (Dodrecht: Reidel), p. 105.
- Kane, S. R., Feinmore, E. E., Klebesadel, and Laros, J. G. 1988, *Ap. J.* **326**, 1017.
- Langer, S. H., and Petrosian, V. 1977, *Ap. J.* **215**, 666.
- Leach, J., and Petrosian, V. 1983, *Ap. J.* **269**, 715.
- Petrosian, V. 1985, *Ap. J.*, **299**, 987.
- Rieger, E., Reppin, C., Kanbach, G., Forrest, D. J., Chupp, E. L., and Share, G. H. 1983, in *18th Int. Cosmic Ray Conf.*, Bangalore, **10**, 338.
- Vestrand, W. T., Forrest, D. J., Chupp, E. L., Rieger, E., and Share, G. H. 1987, *Ap. J.*, **322**, 1010.

FIGURE CAPTIONS

Fig. 1---Correlation diagram between HXRBS total counts and GRS fluences. The solid line is the least square fit to the solid dots representing disk flares; the dashed line, "+" marks representing limb flares. See the text for details.

Fig. 2---Normalized GRS fluence vs. heliocentric angle. GRS fluences are normalized with respect to HXRBS total counts. The solid line is the best fit to the data.

Fig. 3---Center-to-limb variation. Two cases of Dermer and Ramaty's calculations are shown together with two straight lines having the same slope as the regression in Figure 2.

Fig. 4---Correlation diagram between HXRBS total counts and GRS fluences with the center-to-limb variation removed.

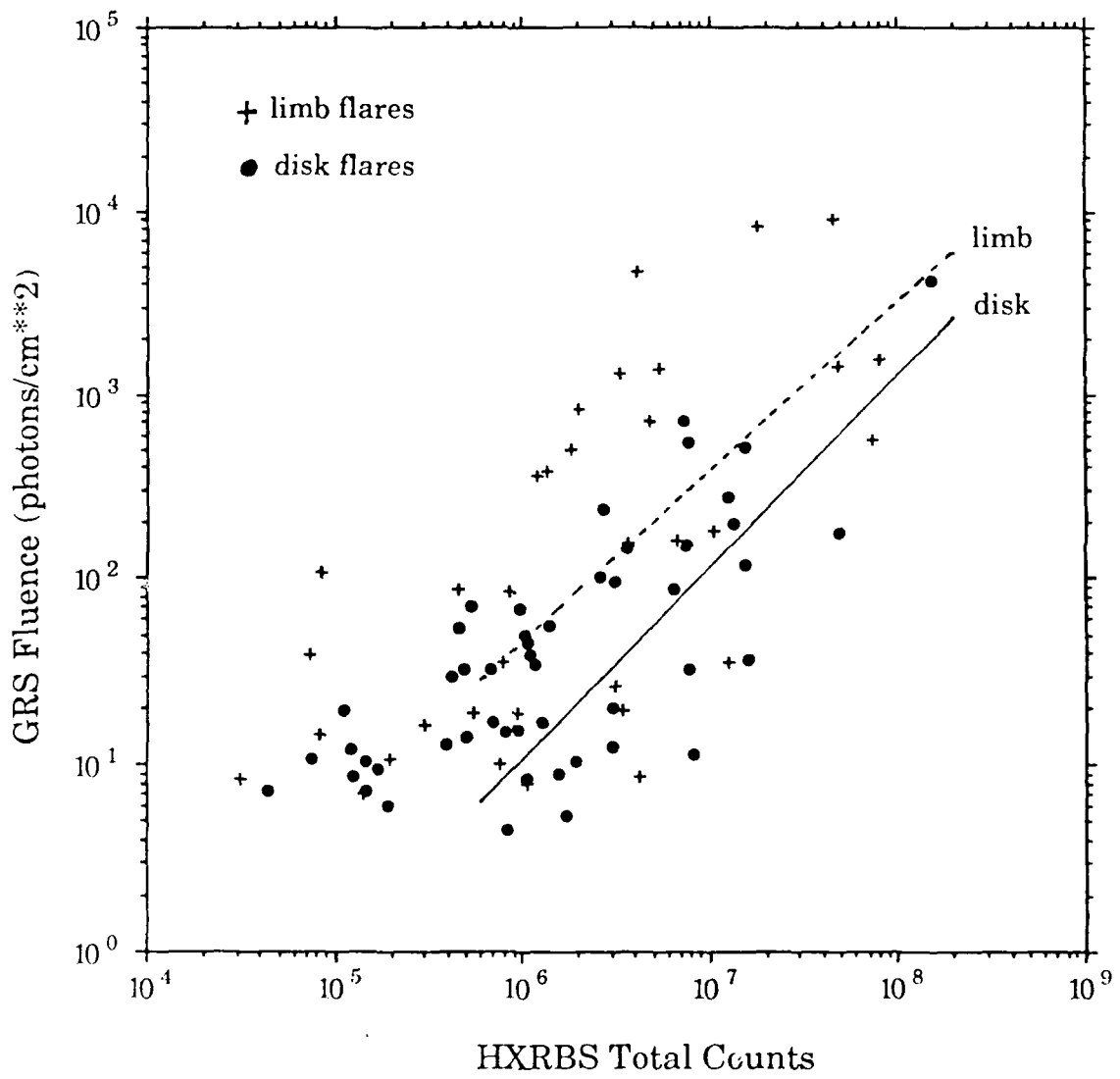


Fig. 1

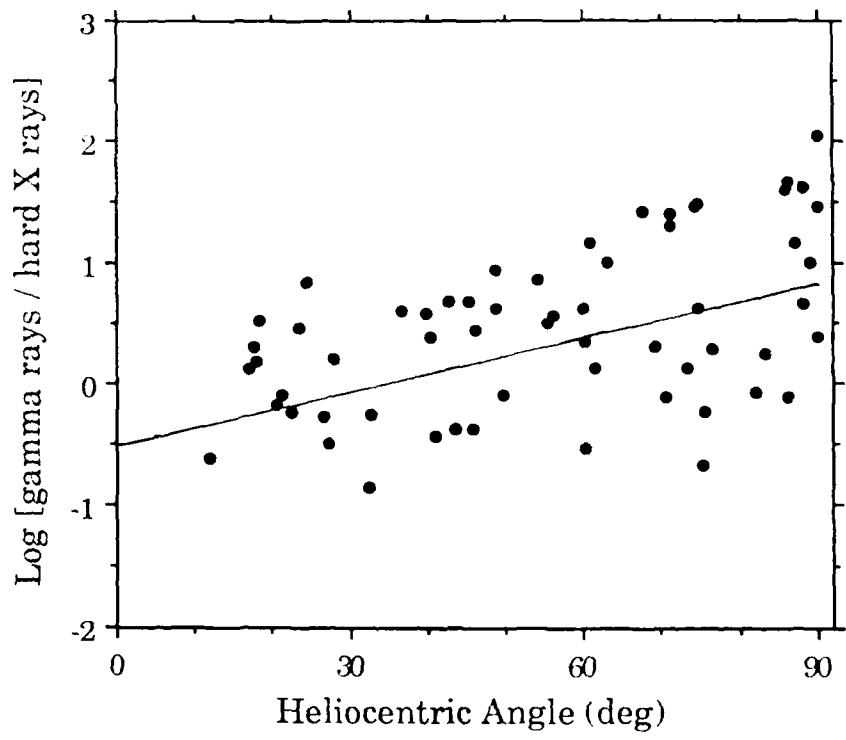


Fig. 2

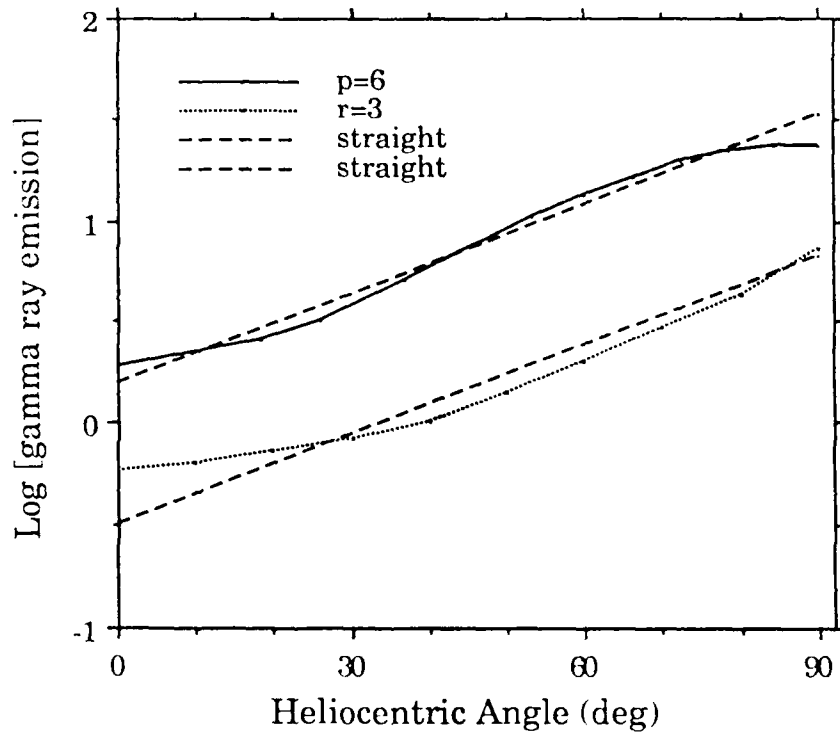


Fig. 3

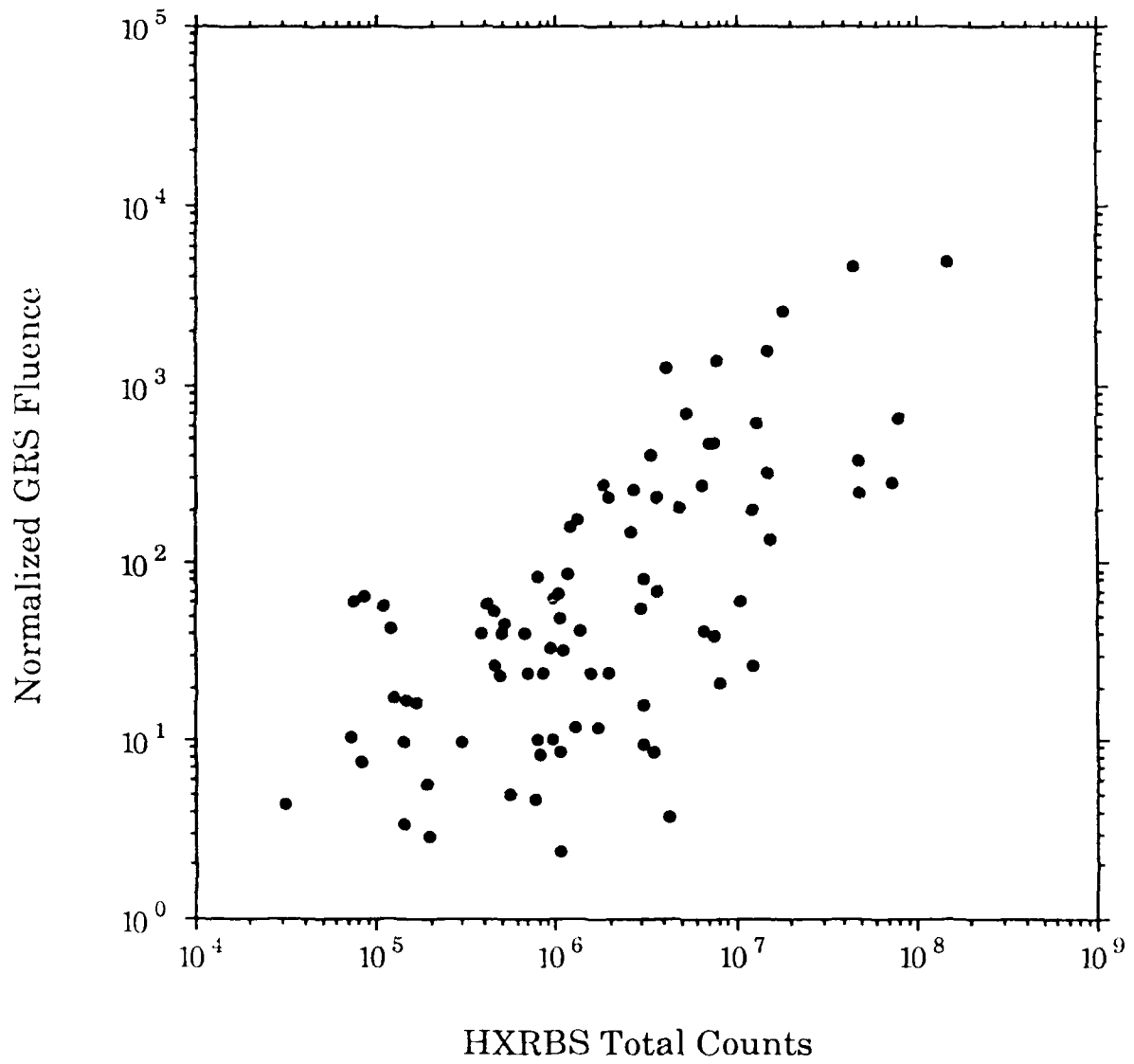


Fig. 4